Electronic Supplementary Material (ESI) for Journal of Materials Chemistry C.

Electronic Supplementary Material (ESI) for Journal of Materials Chemistry C.
This journal is © The Royal Society of Chemistry 2020

Supporting Information for

High performance gas sensors with dual response based on organic ambipolar transistors

Xu Zhou, Zi Wang, Ruxin Song, Yadan Zhang, Lunan Zhu, Di Xue, Lizhen Huang* and Lifeng Chi*

Jiangsu Key Laboratory for Carbon-Based Functional Materials & Devices, Institute of Functional Nano & Soft Materials (FUNSOM), Joint International Research Laboratory of Carbon-Based Functional Materials and Devices, Soochow University, 199 Ren'ai Road, Suzhou, 215123, Jiangsu, PR China

*Corresponding author. E-mail: chilf@suda.edu.cn, lzhuang@suda.edu.cn. Fax: +86-512-65880725. Tel.: +86-512-65880725

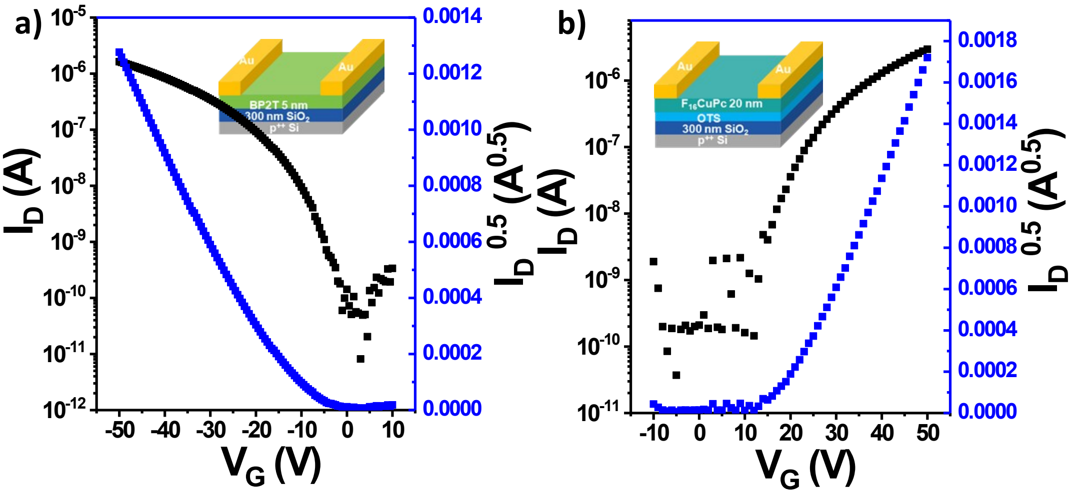

Figure S1. Device configuration of the unipolar transistors and typical transfer characteristic curve of a) BP2T, b) OTS-F_{16}CuPc.

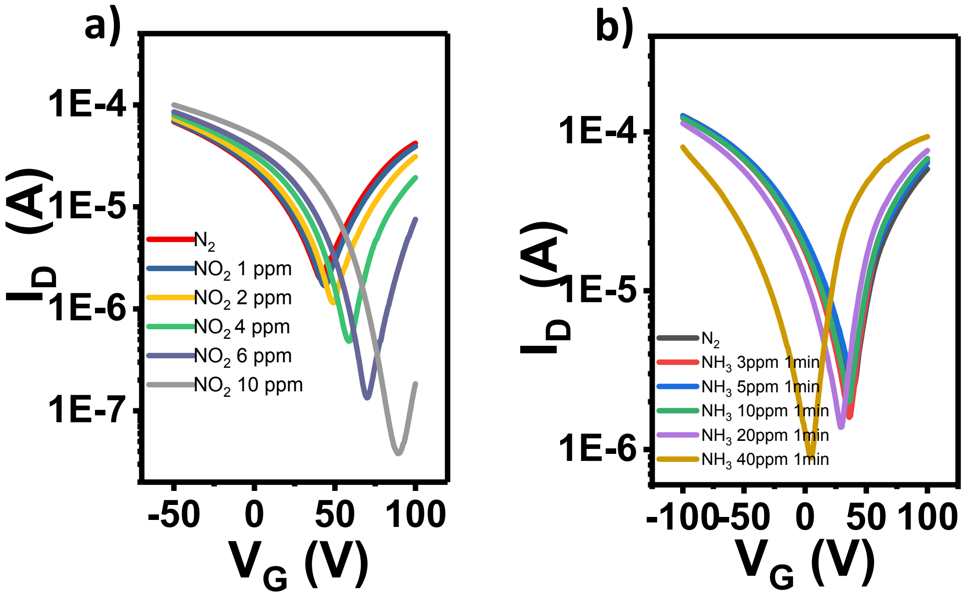

Figure S2. Responses of the ambipolar OFET-based sensors in n-channel transport upon exposure to different vapors at various concentrations. Transfer curves of ambipolar transistor under exposure to a) NO_2, b) NH_3 at different concentrations.

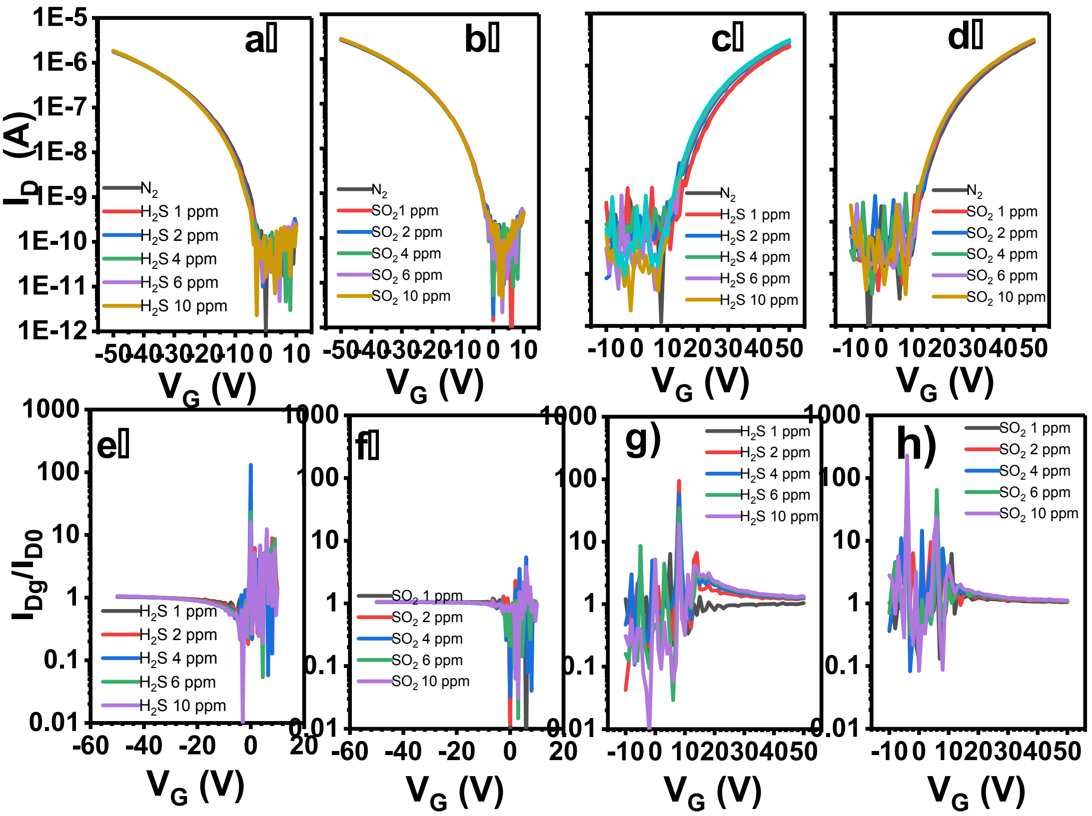

Figure S3. Responses of the unipolar OFET-based sensors upon exposure to different vapors at various concentrations. (a-b) Transfer curves of BP2T under exposure to a) H_2S, b) SO_2 at different concentrations; (c-d) Transfer curves of $F_{16}CuPc$ under exposure to c) H_2S, d) SO_2 at different concentrations; (e-f) The responsivity (I_{Dg}/I_{D0}) of BP2T OFET with various e) H_2S, f) SO_2 concentrations; (g-h) The responsivity (I_{Dg}/I_{D0}) of $F_{16}CuPc$ with various e) H_2S, f) SO_2 concentrations.

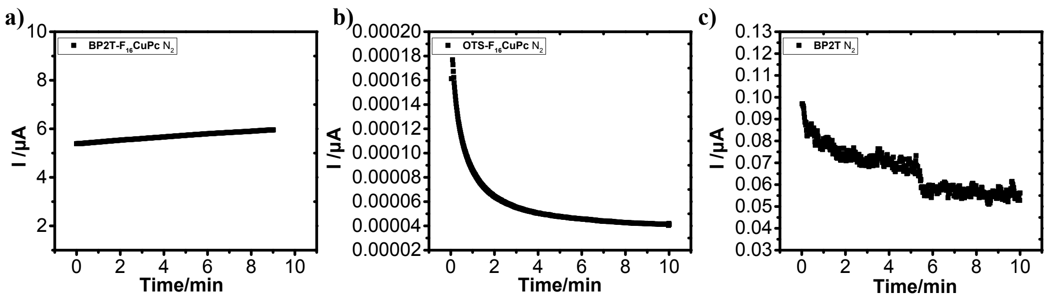

Figure S4 The voltage bias stability of ambipolar and unipolar transistors. a)

BP2T/F_{16}CuPc ambipolar transistor, b) F16CuPc unipolar transistor, c) BP2T unipolar transistor.

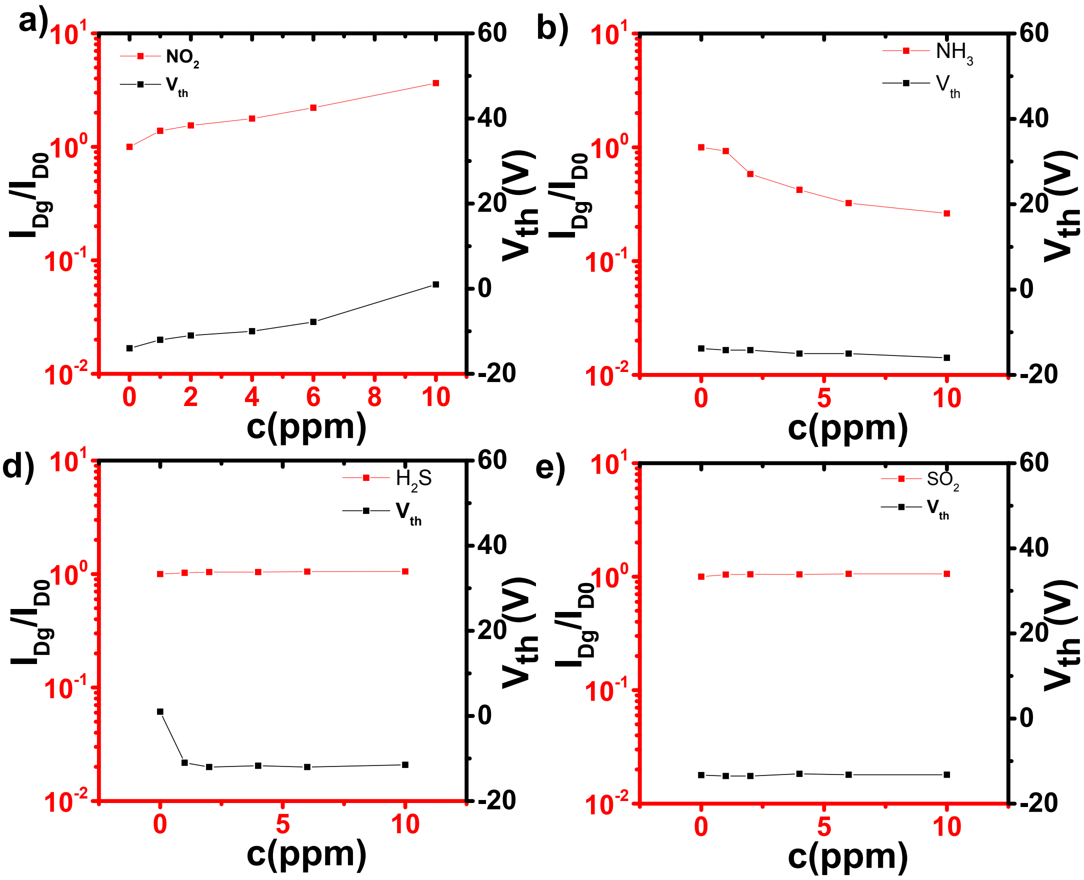

Figure S5. Sensing performance of BP2T OFET-based sensors upon exposure to different vapors. (a-d) the responsivity R (I_{Dg}/I_{D0}) at gate voltage = -50 V and the shift of V_{th} as the function with various a) NO_2, b) NH_3, c) H_2S, d) SO_2 concentrations.

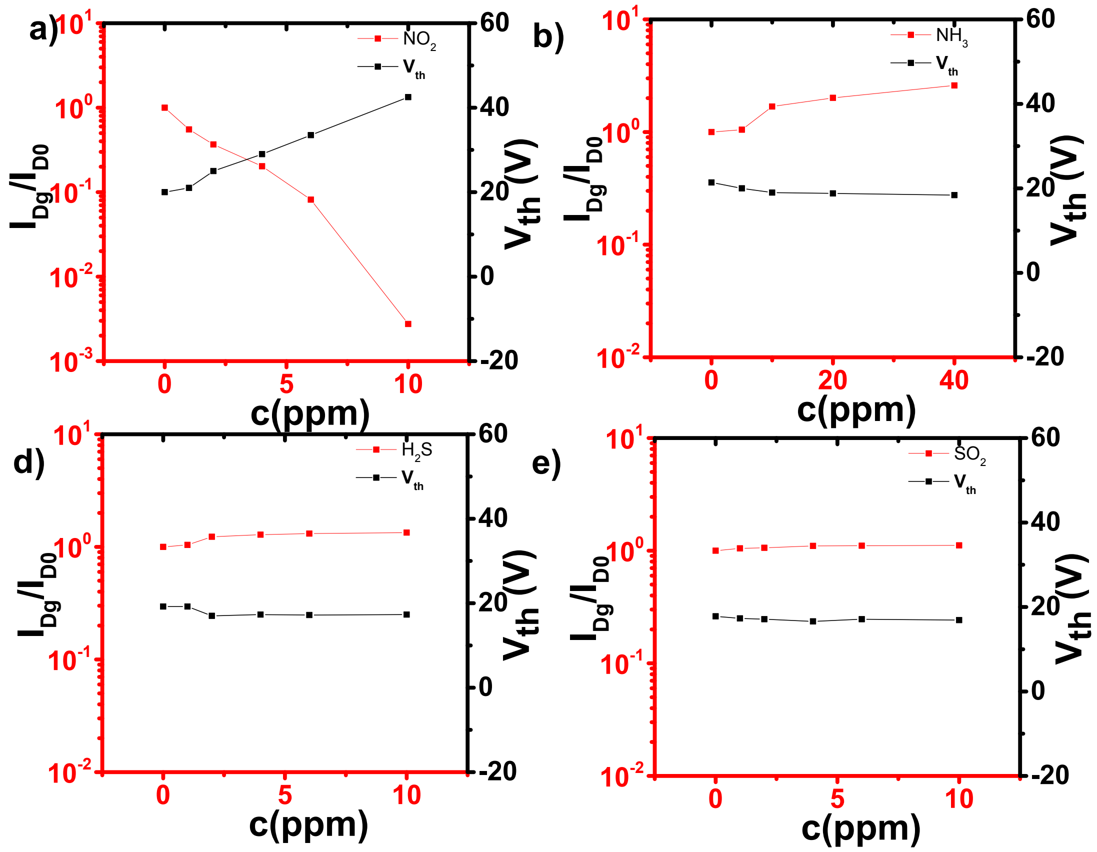

Figure S6. Sensing performance of OTS-F_{16}CuPc OFET-based sensors upon exposure to different vapors. (a-d) the responsivity R (I_{Dg}/I_{D0}) at gate voltage = 50 V and the shift of V_{th} as the function with various a) NO_2, b) NH_3, c) H_2S, d) SO_2 concentrations.

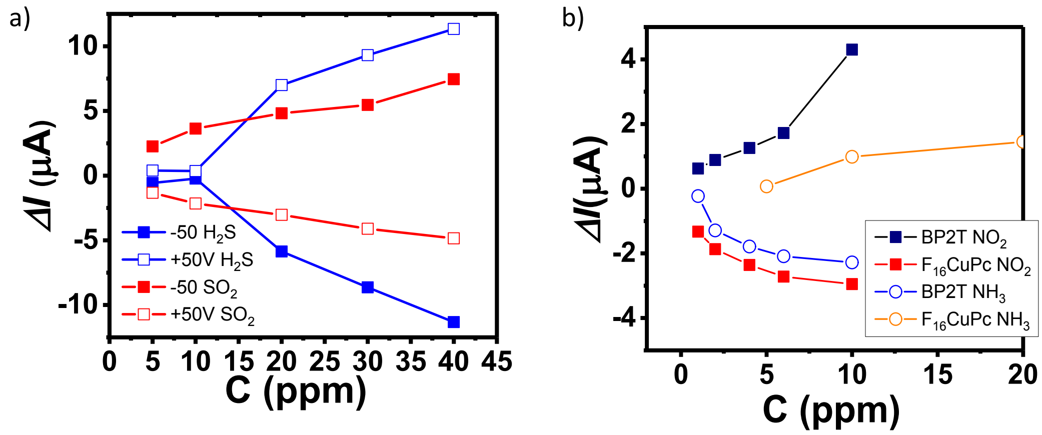

Figure S7. Responses of a) ambipolar b) unipolar OFET-based sensors upon exposure to different vapors. a) the I_D changes at gate voltage = -50 V and 50 V with different concentrations of H_2S and SO_2. b) the I_D changes at gate voltage = -50 V for BP2T and 50 V for OTS-F16CuPc with different concentrations of NH_3 and NO_2.

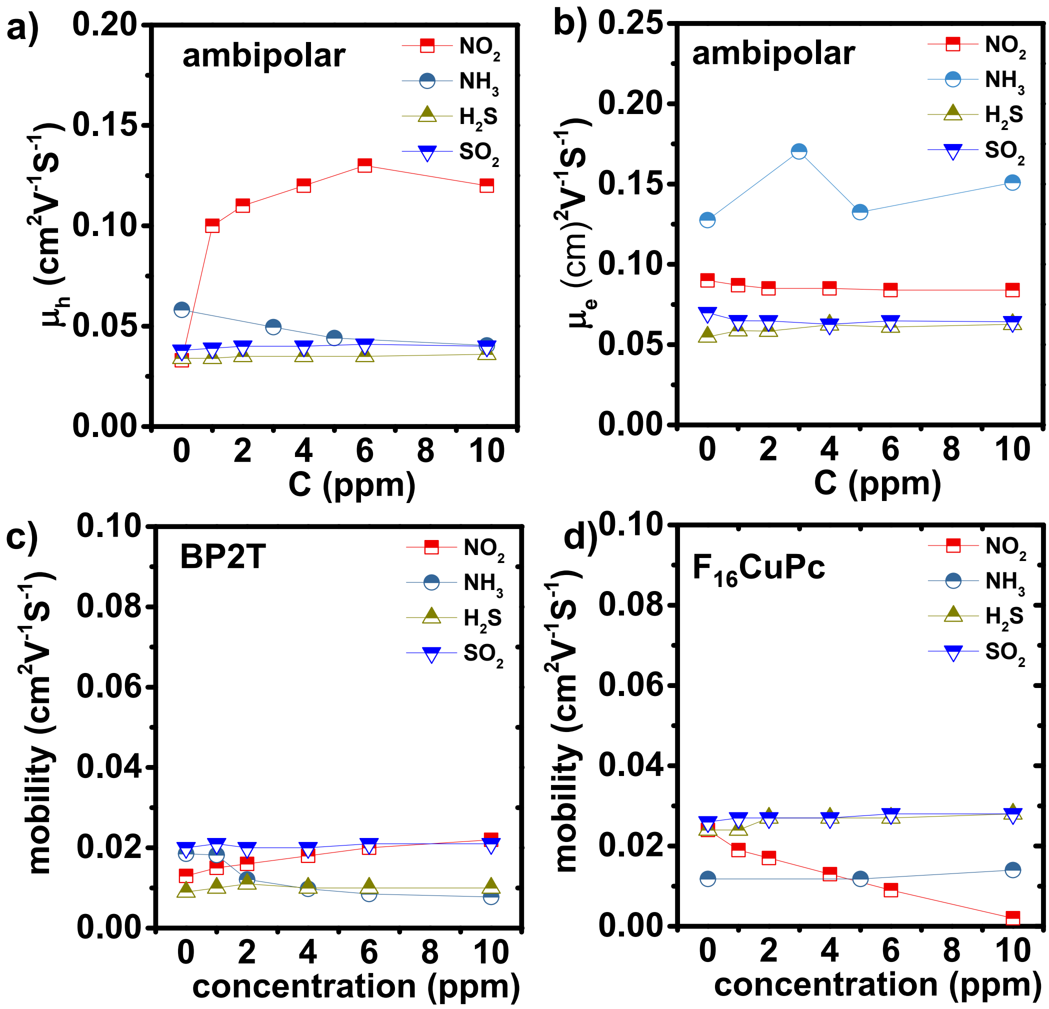

Figure S8. Charge mobility evolution with the gas concentration of the series of transistors. a) Hole and b) electron charge mobility of ambipolar OFET. (c-d) Charge mobility of c) BP2T OFET d) OTS-F_{16}CuPc OFET as the function with various gas concentrations.

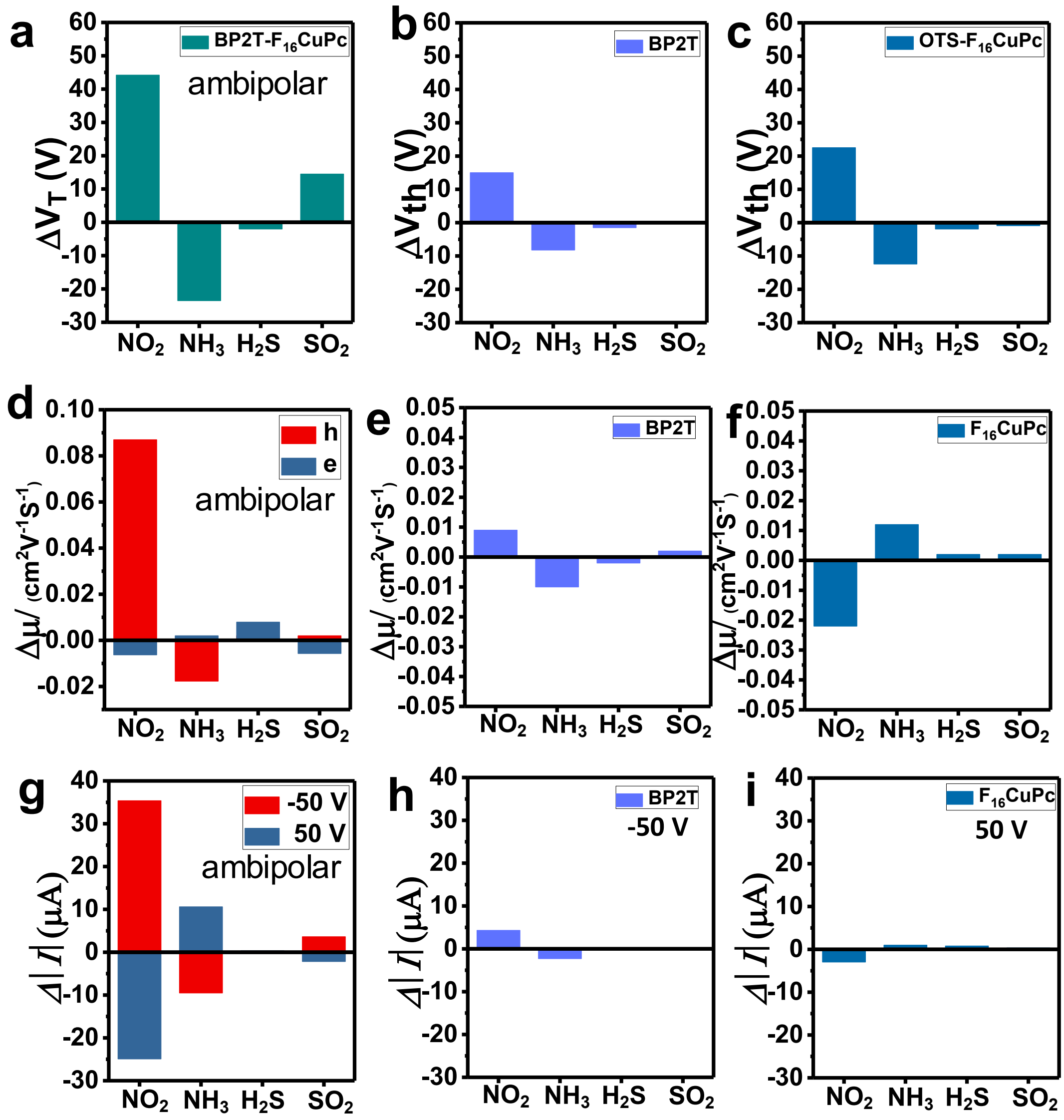

Figure S9. (a-c) V_T shifting of a) ambipolar OFET device, b) V_{th} shifting of BP2T based OFET device, c) V_{th} shifting of F_{16}CuPc based OFET device in response to four gases; (d-f) charge mobility changes and (g-i) saturation current changes of d, g) ambipolar, e, h) BP2T, f, i) F_{16}CuPc in exposure to 10 ppm NO_2, 40 ppm NH_3, H_2S and SO_2.